International Journal of Biochemistry and Cell Biology 107 (2019) 82–91

Contents lists available at ScienceDirect

International Journal of Biochemistry and Cell Biology

journal homepage: www.elsevier.com/locate/biocel

Protective effects of tanshinone IIA on SH-SY5Y cells against oAβ_{1-42}-induced apoptosis due to prevention of endoplasmic reticulum stress

Weina Yang[a], Jianshui Zhang[a], Lili Shi[b], Shengfeng Ji[a], Xiaohua Yang[c], Wanying Zhai[a], Hangfan Zong[a], Yihua Qian[a,*]

[a] Department of Human Anatomy, Histology and Embryology, School of Basic Medical Sciences, Xi'an Jiaotong University Health Science Center, 76 Yanta West Road, Xi'an, 710061, China
[b] Department of Human Anatomy, Xi'an Medical University, 1 Xinwang road, Xi'an, 710021, China
[c] Key Laboratory of Ministry of Health for Forensic Sciences, School of Forensic Sciences, Xi'an Jiaotong University Health Science Center, 76 Yanta West Road, Xi'an, 710061, China

ARTICLE INFO

Keywords:
Alzheimer disease
Tanshinone IIA
β-amyloid protein
Endoplasmic reticulum stress
Apoptosis

ABSTRACT

Endoplasmic reticulum (ER) stress caused by β-amyloid protein (Aβ) may play an important role in the pathogenesis of Alzheimer disease (AD). Our previous data have indicated that tanshinone IIA (tan IIA) protected primary neurons from Aβ induced neurotoxicity. To further explore the neuroprotection of tan IIA, here we study the effects of tan IIA on the ER stress response in oligomeric Aβ_{1-42} (oAβ_{1-42})-induced SH-SY5Y cell injury. Our data showed that tan IIA pretreatment could increase cell viability and inhibit apoptosis caused by oAβ_{1-42}. Furthermore, tan IIA markedly suppressed ER dilation and prevented oAβ_{1-42}-induced abnormal expression of glucose regulated protein 78 (GRP78), initiation factor 2α (eIF2α), activating transcription factor 6 (ATF6), as well as inhibited the activation of C/EBP homologous protein (CHOP) and c-Jun N-terminal kinase (JNK) pathways. Moreover, tan IIA ameliorated oAβ_{1-42}-induced Bcl-2/Bax ratio reduction, prevented cytochrome *c* translocation into cytosol from mitochondria, reduced oAβ_{1-42}-induced cleavage of caspase-9 and caspase-3, suppressed caspase-3/7 activity, and increased mitochondrial membrane potential (MMP) and ATP content. Meanwhile, oAβ_{1-42}-induced cell apoptosis and activation of ER stress can also be attenuated by the inhibitor of ER stress 4-phenylbutyric acid (4-PBA). Taken together, these data indicated that tan IIA protects SH-SY5Y cells against oAβ_{1-42}-induced apoptosis through attenuating ER stress, modulating CHOP and JNK pathways, decreasing the expression of cytochrome *c*, cleaved caspase-9 and cleaved caspase-3, as well as increasing the ratio of Bcl-2/Bax, MMP and ATP content. Our results strongly suggested that tan IIA may be effective in treating AD associated with ER stress.

1. Introduction

Alzheimer's disease (AD) is a common dementia in the elderly. Two major hallmarks, senile plaques (SPs) and neurofibrillary tangles (NFTs), are widely known to be characteristic of AD pathology. NFTs consist of hyperphosphorylated tau protein in neurons, and SPs consist of β-amyloid protein (Aβ) in the extracellular space. Several hypotheses have been currently proposed to elucidate AD pathogenesis, and Aβ hypothesis is accepted as one of the most evidence-based (Ferreira and Klein, 2011; Musiek and Holtzman, 2015). Accumulation of Aβ in the brain leads to a series of harmful events including plaque formation, tau hyperphosphorylation, oxidative stress, endoplasmic reticulum (ER) stress and eventually neuronal apoptosis (Chen et al., 2017; Gerakis and Hetz, 2017; Guo et al., 2018; Hardy and Allsop, 1991; Lim and Han, 2018; Yao et al., 2017).

The ER is the main compartment involved in protein folding and secretion and is drastically affected in AD neurons. The accumulation of unfolded or misfolded proteins in the ER activates a cellular stress response known as the unfolded protein response (UPR) and initiates the removal of toxic misfolded proteins as a way to protect the cell (Gerakis and Hetz, 2017; Hosoi et al., 2009). The UPR is initiated by three stress sensor proteins, including inositol requiring enzyme 1 (IRE1), (PKR)-like endoplasmic reticulum kinase (PERK), and activating transcription factor 6 (ATF6). These are normally maintained in an inactive state via binding with an ER chaperone, glucose regulated protein 78 (GRP78). However, ER stress triggers the release of GRP78 from the complexes, and the stress sensors recognize the misfolded proteins in the ER and activate a complex signaling network of UPR (Bertolotti et al., 2000).

* Corresponding author.
E-mail address: qianyh38@mail.xjtu.edu.cn (Y. Qian).

https://doi.org/10.1016/j.biocel.2018.12.011
Received 19 July 2018; Received in revised form 6 December 2018; Accepted 18 December 2018
Available online 19 December 2018
1357-2725/

For example, extended phosphorylation of PERK subsequently induces the phosphorylation of α subunit of eukaryotic translation initiation factor (eIF2α) at ser51. Phosphorylated eIF2α also promotes the translation of mRNAs such as ATF4 (Duran-Aniotz et al., 2014; Urra et al., 2013). ATF4 acts as the upstream activator of genes involved in amino acid metabolism and transportation, as well as genes related to apoptosis, including C/EBP homologous protein (CHOP) and members of the B-cell lymphoma 2 (Bcl-2) protein family (Chen et al., 2018; Gu et al., 2010; Vattem and Wek, 2004).

Recently, soluble oligomeric Aβ (oAβ) were reported to be more highly toxic to synapses than fibrillary Aβ (fAβ) (Evans et al., 2008; Kittelberger et al., 2012; Sakono and Zako, 2010). oAβ may be formed early on in the disease process both inside and outside synaptic terminals (Kokubo et al., 2005; Takahashi et al., 2004), and intracellular and extracellular Aβ may interact (LaFerla et al., 2007; Oddo et al., 2006). Previous studies indicated that oAβ, but not fAβ, induced cell apoptotic death by activating ER stress (Chafekar et al., 2007; Costa et al., 2012). Data from *in vitro* and *in vivo* experiments confirmed that Aβ promotes the expression of the markers of ER stress and increases the level of effectors of ER stress related apoptosis pathways such as CHOP, c-Jun N-terminal kinase (JNK), and caspase-12 (Barbero-Camps et al., 2014; Song et al., 2003; Tseng et al., 2008). In contrast, blockage of ER stress is indicated to effectively ameliorate cells damage induced by Aβ (Lee et al., 2010). These data demonstrate that ER stress is one of the significant molecular mechanisms involved in Aβ cytotoxicity.

There have been continuous efforts to develop drugs or nutraceuticals to treat or prevent AD. Numerous candidate treatment agents have been examined, including various kinds of herbal and natural products. Tanshinone IIA (tan IIA) is an active lipophilic component extracted from the root of *Salvia miltiorrhiza* Bunge (Danshen) and exerts multiple neuroprotective potentials relevant to AD, such as anti-Aβ, antioxidant, anti-inflammation, anti-apoptosis, and acetylcholinesterase inhibition (Akaberi et al., 2016; Dong et al., 2012; Jeon et al., 2011; Jiang et al., 2014; Kong et al., 2017; Liu et al., 2016; Maione et al., 2017; Seo et al., 2017; Wang et al., 2013) (Fig. 1). Our previous study demonstrated that pretreatment of tan IIA protected primary neurons from $A\beta_{25-35}$ induced neurotoxicity, reduced the cleavage of p35 into p25 and thus inhibited the cyclin-dependent kinase 5 pathway. Additionally, the compound can significantly reduce phosphorylated tau levels in neurons and improve the impairment of the cell ultrastructure, including nuclear condensation, fragmentation, and neurofibril collapse (Shi et al., 2012). In addition, we found that tan IIA also suppresses $A\beta_{1-42}$ induced apoptosis in cortical neurons by activating the Bcl-xL pathway (Qian et al., 2012). Recently, our experimental data confirmed that tan IIA prevents streptozotocin (STZ) induced memory deficits in mice (Liu et al., 2016). It has been proposed that tan IIA protects SH-SY5Y cells against glutamate toxicity by reducing oxidative stress and regulating apoptosis and MAPK pathways (Li et al., 2017). Moreover, tan IIA enhanced insulin sensitivity and improved glucose metabolic disorders by attenuating ER stress induced insulin resistance in L6 myotubes mice (Hwang et al., 2012). Tan IIA also significantly attenuated oxidative stress injury and decreased ER stress mediated apoptosis in the protection of kidney hypothermic preservation (Zhang et al., 2012). However, the effects of tan IIA on ER stress mediated apoptosis in AD are lacking. Therefore, in the present study, we investigate the potentially beneficial effects of tan IIA on preventing ER stress and apoptosis induced by $oA\beta_{1-42}$ in SH-SY5Y cells and attempted to explore its underlying mechanisms.

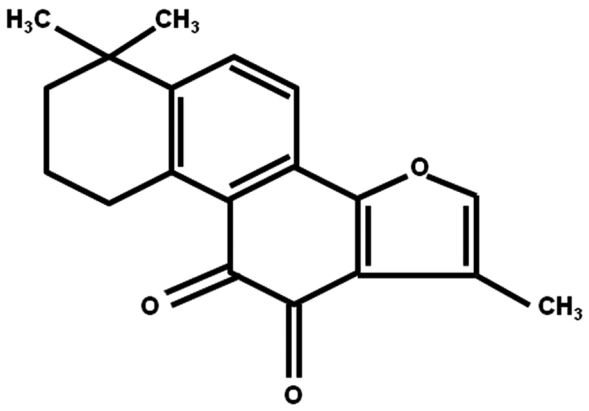

Fig. 1. Chemical structure of tan IIA.

2. Materials and methods

2.1. Reagents and antibodies

See Supplementary data.

2.2. Cell culture

Human neuroblastoma SH-SY5Y cells was cultured in high glucose DMEM supplemented with 10% (v/v) FBS, penicillin (100 units/mL), streptomycin (100 μg/mL), and L-glutamine (2 mM) at 37 °C in a humidified incubator under an atmosphere of 95% air and 5% CO_2. At 70–80% confluence, cells were maintained in serum-free conditions overnight prior to experiments.

2.3. Preparation of $oA\beta_{1-42}$ and tan IIA

Preparation of $oA\beta_{1-42}$ was carried out as previously described (Cai et al., 2014). Briefly, solid $A\beta_{1-42}$ peptide was dissolved at a concentration of 1 mg/mL in cold HFIP and then incubated at room temperature for at least 1 h to establish monomerization and randomization of structure. The peptide was separated into aliquots in sterile microcentrifuge tubes and freeze-dried for 3 h. When the film is formed, it was stored at −80 °C. To oligomerize Aβ, the peptide was first resuspended in anhydrous DMSO to a concentration of 2 mM. Next, the solution was diluted with DMEM to the appropriate concentration and incubated for 24 h at 4 °C (Choi et al., 2017; Chromy et al., 2003; Dahlgren et al., 2002).

Tan IIA was dissolved in DMSO (no more than 0.1% in v/v), and was further dissolved in DMEM.

2.4. MTT reduction assay to evaluate cell viability

Cell viability was measured and calculated using the MTT reduction assay, as described previously (Shi et al., 2012; Yang et al., 2015) (see Supplementary data).

2.5. Detection of apoptosis by TUNEL

See Supplementary data.

2.6. Transmission electron microscopy

The ultrastructural characteristics of cells suffered from ER stress or control cells were visualized via transmission electron microscopy (see Supplementary data).

2.7. Immunofluorescence assay

To investigate the location of protein expression, we performed immunofluorescence staining analysis. See Supplementary data.

2.8. Semiquantitative reverse transcription polymerase chain reaction (RT-PCR)

See Supplementary data.

2.9. Isolation of mitochondrial and cytosolic fractions

The mitochondrial and cytosolic fractions of cells were separated using mitochondria isolation kit for cultured cells according to manufacturer's instructions.

2.10. Mitochondrial membrane potential (MMP) assay

MMP was measured using JC-1, a dual-emission dye, as previously described (Hu et al., 2016) (see Supplementary data).

2.11. Detection of mitochondrial ATP level

ATP levels were measured in isolated mitochondria from all groups of cells using ATP luminescent assay kit (see Supplementary data).

2.12. Caspase-3/7 activity assay

Caspase-3/7 activity was determined using the Caspase-Glo 3/7 kit according to the manufacturer's protocols (see Supplementary data).

2.13. Western blotting analysis

Western blotting was performed as described previously (Yang et al., 2015) (see Supplementary data).

2.14. Statistical analysis

Results were analyzed with SPSS 13.0 software and presented as mean ± standard deviation (SD) from at least three independent experiments. Statistical significance among different experimental groups were determined by one-way analysis of variance (ANOVA) followed by Newman–Keuls or Tukey–Kramer test, and $p < 0.05$ was considered significant for all analyses.

3. Results

3.1. Tan IIA protected SH-SY5Y cells against oAβ_{1-42}-induced toxicity

To investigate the toxic of oAβ_{1-42}, SH-SY5Y cells were exposed to oAβ_{1-42} (ranging from 1 μM to 20 μM) for 24 h and the cell viability was assessed by the MTT reduction assay. As shown in Fig. 2A, oAβ_{1-42} treatment caused a significant decrease of cell viability in SH-SY5Y cells and the cytotoxic effect of oAβ_{1-42} exhibited a dose-dependent manner. The viability of the cell was decreased approximately 47% after treating with 5 μM oAβ_{1-42} for 24 h. Based on the results, 5 μM was selected as the optimal oAβ_{1-42} concentrations for subsequent experiments. We then examined the neuroprotective effects of tan IIA on oAβ_{1-42}-induced toxicity in SH-SY5Y cells. The MTT assay showed that cell viability was not significantly reduced by the low concentrations of tan IIA (0.1 μM to 20 μM), but was significantly decreased by the higher concentration of tan IIA (40 μM), suggesting that tan IIA at the concentration of < 20 μM induced no toxicity to SH-SY5Y cells (Fig. 2B). Furthermore, pretreatment with tan IIA (1, 5, and 10 μM) for 30 min and then treated with 5 μM oAβ_{1-42} for 24 h significantly increased the viability of cells against oAβ_{1-42}-induced cytotoxicity and reached the maximum effect at 5 μM. However, lower dose (0.1 μM) tan IIA exhibited no protective effect and treatment with a higher amount (40 μM) of tan IIA increased the cytotoxicity of oAβ_{1-42} ($p < 0.05$ or $p < 0.01$). Moreover, we found that 4-PBA could significantly improve cell viability in oAβ_{1-42} treated SH-SY5Y cells (Fig. 2C). As shown in Fig. 2D, the protective effects of tan IIA on oAβ_{1-42}-induced growth inhibition was further confirmed by observing cells' morphology under a microscope. The results showed that morphology of oAβ_{1-42}-induced cells were obviously damaged and SH-SY5Y cells exposed to oAβ_{1-42} exhibited cell shrinkage, suspending and shape irregularity. However, tan IIA (1, 5 or 10 μM) could protect SH-SY5Y cells against structural damage induced by oAβ_{1-42}.

3.2. Tan IIA rescued oAβ_{1-42}-induced apoptosis in SH-SY5Y cells

To determine whether tan IIA can inhibit oAβ_{1-42}-induced cell apoptosis, we observed the nuclear morphologic changes associated with apoptosis by TUNEL staining. The representative photomicrographs showed that the TUNEL-positive cells as brown localized in SH-SY5Y cells (Fig. 3A). The number of apoptotic cells was increased more than 17-fold after 24 h incubation with 5 μM oAβ_{1-42} compared to controls ($p < 0.01$). However, the number of TUNEL-positive nuclei was significantly reduced when cells were pretreated with tan IIA. At concentrations of 1, 5 and 10 μM, tan IIA reduced the apoptosis of oAβ_{1-42} treated cells to 37.75%, 27.68% and 32.57%, respectively. Similar to tan IIA, 4-PBA also attenuated the apoptosis in oAβ_{1-42} treated SH-SY5Y cells (Fig. 3B) ($p < 0.05$ or $p < 0.01$).

3.3. Effects of tan IIA on the morphological structure of SH-SY5Y cells incubated with oAβ_{1-42}

In eukaryotic cells, the ER is responsible for protein synthesis, folding and maturity, but it also acts as a sensor for cellular stress. In the present study, we examined whether 5 μM of oAβ_{1-42} for 24 h has the

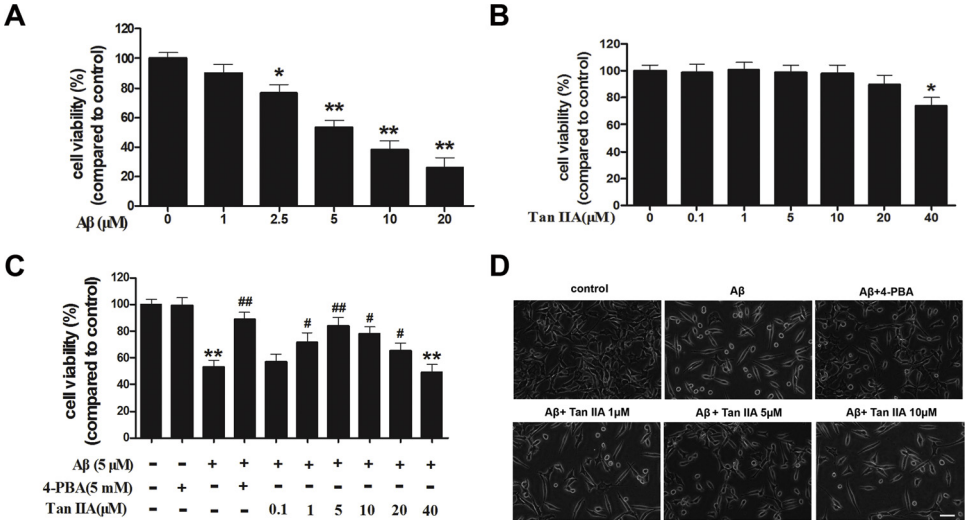

Fig. 2. Protective effects of tan IIA on oAβ_{1-42}-induced toxicity in SH-SY5Y cells. (A) SH-SY5Y cells were untreated (control) or treated with oAβ_{1-42} at 1, 2.5, 5, 10 and 20 μM for 24 h. (B) SH-SY5Y cells were treated with tan IIA at 0.1, 1, 5, 10, 20, and 40 μM for 24 h. (C) SH-SY5Y cells were pretreated with tan IIA (0.1, 1, 5, 10, 20, and 40 μM) for 30 min or pretreated with 4-PBA (5 mM) for 6 h and then incubated with oAβ_{1-42} (5 μM) for an additional 24 h. (D) Morphological characteristics of SH-SY5Y cells were visualized with microscopic analysis. Scale bar is 50 μm. Cell viability was determined by MTT assay. Percentage of cell viability was relative to the untreated control cells. Results were shown as the mean ± SD. The experiments were repeated three times independently. $^{*}p < 0.05$ and $^{**}p < 0.01$ versus control, $^{\#}p < 0.05$ and $^{\#\#}p < 0.01$ versus oAβ_{1-42} treated cells.

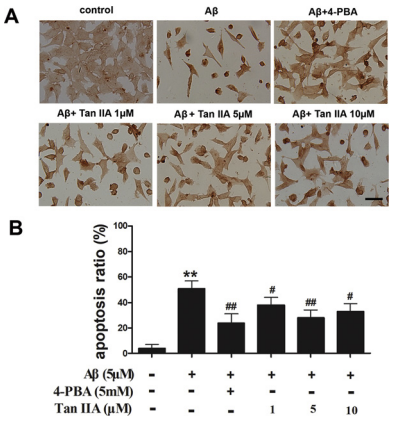

Fig. 3. Tan IIA rescued oAβ_{1-42}-induced apoptosis in SH-SY5Y cells. Cells were pretreated with tan IIA (1, 5, and 10 μM) for 30 min or 4-PBA (5 mM) for 6 h followed by 5 μM oAβ_{1-42} for 24 h. (A) Representative images of TUNEL staining. Scale bar is 50 μm. (B)The ratio was calculated by counting the percentage of cells exhibiting positive TUNEL staining. Results were shown as the mean ± SD. The experiments were repeated three times independently. $^{**}p < 0.01$ versus control, $^{\#}p < 0.05$ and $^{\#\#}p < 0.01$ versus oAβ_{1-42} treated cells.

potential to induce ER stress in SH-SY5Y cells by testing the endoplasmic reticular ultrastructural changes. As shown in Fig. 4, SH-SY5Y cells treated with oAβ_{1-42} presented obvious endoplasmic reticular proliferation, dilation and degranulation, accompanied with some apoptosis characteristic ultrastructural features including chromatin condensation and appearance of chromatin crescent. However, the damage of ER induced by ER stress could be attenuated when cells were preincubated with tan IIA (5 μM) or 4-PBA. These results indicated that tan IIA could attenuate the excessive ER stress.

3.4. Tan IIA prevented oAβ_{1-42}-induced core protein of ER stress expression in SH-SY5Y cells

To explore the relationship between ER stress and the neuroprotective effects of tan IIA, we detected the expression of GRP78, the central regulator of the ER stress (Ghaderi et al., 2018). As shown in Fig. 5A, the mRNA levels of GRP78 was increased significantly when cells treated with oAβ_{1-42} ($p < 0.01$). However, pretreatment with tan IIA (1, 5 or 10 μM) effectively attenuated the GRP78 mRNA ($p < 0.05$ or $p < 0.01$). Using western blotting analysis, we further found that treatment of cells with 5 μM oAβ_{1-42} for 24 h significantly increased the expression of GRP78 compared with the controls, but this was significantly reduced by tan IIA (1, 5 or 10 μM) pretreatment (Fig. 5B) ($p < 0.05$ or $p < 0.01$). The immunofluorescence staining of GRP78 was consistent with those of western blotting results (Fig. 5C). The effects of 4-PBA on GRP78 expression induced by oAβ_{1-42} was similar to tan IIA. In this experiment, 5 μM tan IIA provided more significant neuroprotection than other dosages.

3.5. Tan IIA suppressed oAβ_{1-42}-induced the expression of UPR signaling protein in SH-SY5Y cells

After the accumulation of misfolded proteins, GRP78 is released to form aggregates with transmembrane signaling proteins, resulting in the initiation of the UPR. The UPR is primarily mediated by three signal pathways: PERK/eIF2α, IRE1/XBP1 and ATF6 pathways (Bertolotti et al., 2000). To further investigate the effects of tan IIA against ER stress induced by oAβ_{1-42} in SH-SY5Y cells, we tested the levels of phospho-eIF2α and ATF6 proteins. As shown in Fig. 6A, the expression of phospho-eIF2α was upregulated significantly when cells exposed to 5 μM oAβ_{1-42} for 24 h, which could be significantly inhibited by tan IIA (1, 5 or 10 μM) pretreatment ($p < 0.01$). ATF6 is cleaved during ER stress and its cytosolic domain translocates to the nucleus (Teodoro et al., 2012). In this study, tan IIA (1, 5 or 10 μM) drastically reduced the protein levels of ATF6 in the nuclear fractions compared to the oAβ_{1-42} group, while the levels of this total protein was no significantly difference in the cells ($p < 0.05$ or $p < 0.01$). In addition, the immunofluorescence staining of ATF6 were consistent with western blotting results (Fig. 6B). The same inhibitory effects on the expression of phospho-eIF2α and ATF6 were observed in 4-PBA pretreated cells. These results showed that ER stress contribute to oAβ_{1-42}-induced SH-SY5Y cell injury, which could be antagonized by tan IIA.

3.6. Tan IIA inhibited oAβ_{1-42}-induced activation of CHOP and JNK pathways in SH-SY5Y cells

When ER stress is excessive and/or prolonged, the initiation of apoptosis is promoted by the transcriptional induction of CHOP, JNK, or the caspase-12 dependent pathway (Sadeghi et al., 2017; Sharma et al., 2012; Tarantino and Caputi, 2011; Urano et al., 2000; Wortel et al., 2017). In this study, we detected the expression of CHOP and phospho-JNK to investigate whether tan IIA inhibited apoptosis induced by ER stress via these two signaling pathways. Using western blotting analysis, we found that treatment of cells with 5 μM oAβ_{1-42} for 24 h significantly enhanced the expression of CHOP, as well as phospho-JNK ($p < 0.01$). On the contrary, tan IIA (1, 5 or 10 μM) suppressed the expression of CHOP and phospho-JNK (Fig. 7A) ($p < 0.05$ or $p < 0.01$) Likewise, the mRNA levels of CHOP and the immunofluorescence staining of CHOP were consistent with western blotting results (Fig. 7B and C). 4-PBA also effectively inhibited the expression of CHOP and phospho-JNK. These results confirmed that tan IIA protectes SH-SY5Y cells from oAβ_{1-42}-induced apoptosis at least partly through suppression of CHOP and JNK pathways.

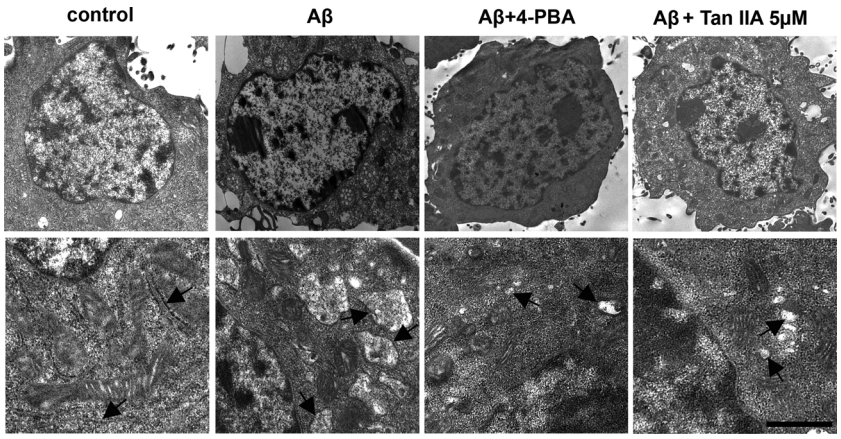

Fig. 4. The morphological endoplasmic reticular ultrastructural changes in SH-SY5Y cells were observed under transmission electric microscopy. Cells were pretreated with tan IIA (5 μM) for 30 min or 4-PBA (5 mM) for 6 h followed by 5 μM oAβ_{1-42} for 24 h. SH-SY5Y cells treated with oAβ_{1-42} displayed endoplasmic reticulum proliferation, dilation and degranulation, accompanied with condensed chromatin and apoptotic nuclei. Scale bar is 1 μm. Arrow indicated endoplasmic reticulum.

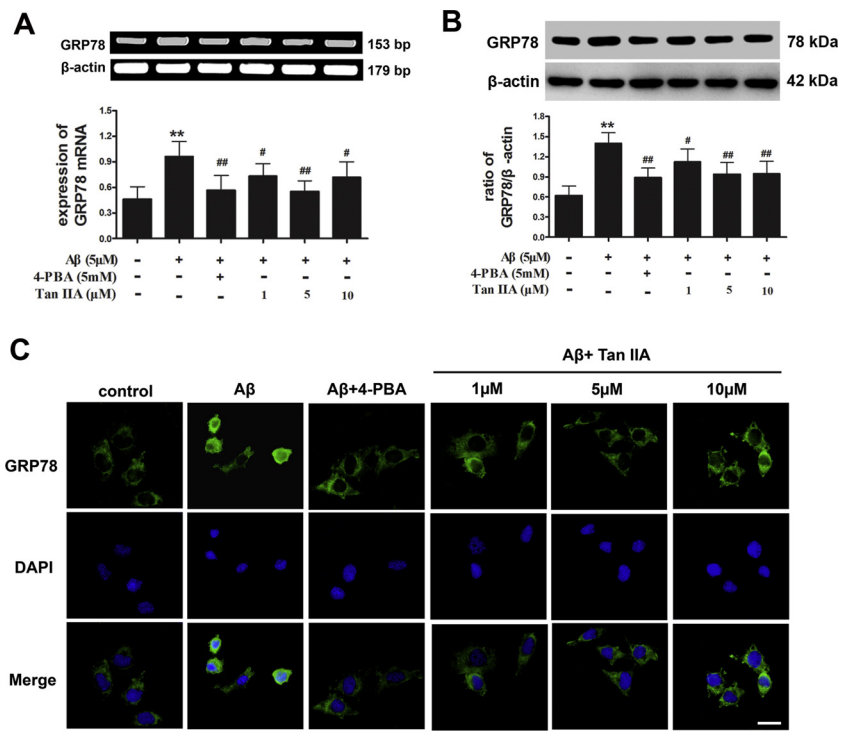

Fig. 5. Tan IIA prevented oAβ_{1-42}-induced the expression of GRP78 in SH-SY5Y cells. Cells were pretreated with tan IIA (1, 5, and 10 μM) for 30 min or 4-PBA (5 mM) for 6 h followed by 5 μM oAβ_{1-42} for 24 h. (A) The mRNA expression of GRP78 with RT-PCR. β-actin was detected for controls. (B) The protein expression of GRP78 with western blotting. β-actin was detected for controls. (C) Immunofluorescence of GRP78 (green), the nuclear (blue) was labelled with DAPI. Scale bar is 20 μm. Results were shown as the mean ± SD. The experiments were repeated three times independently. $^{**}p < 0.01$ versus control, $^{\#}p < 0.05$ and $^{\#\#}p < 0.01$ versus oAβ_{1-42} treated cells. (For interpretation of the references to colour in this figure legend, the reader is referred to the web version of this article).

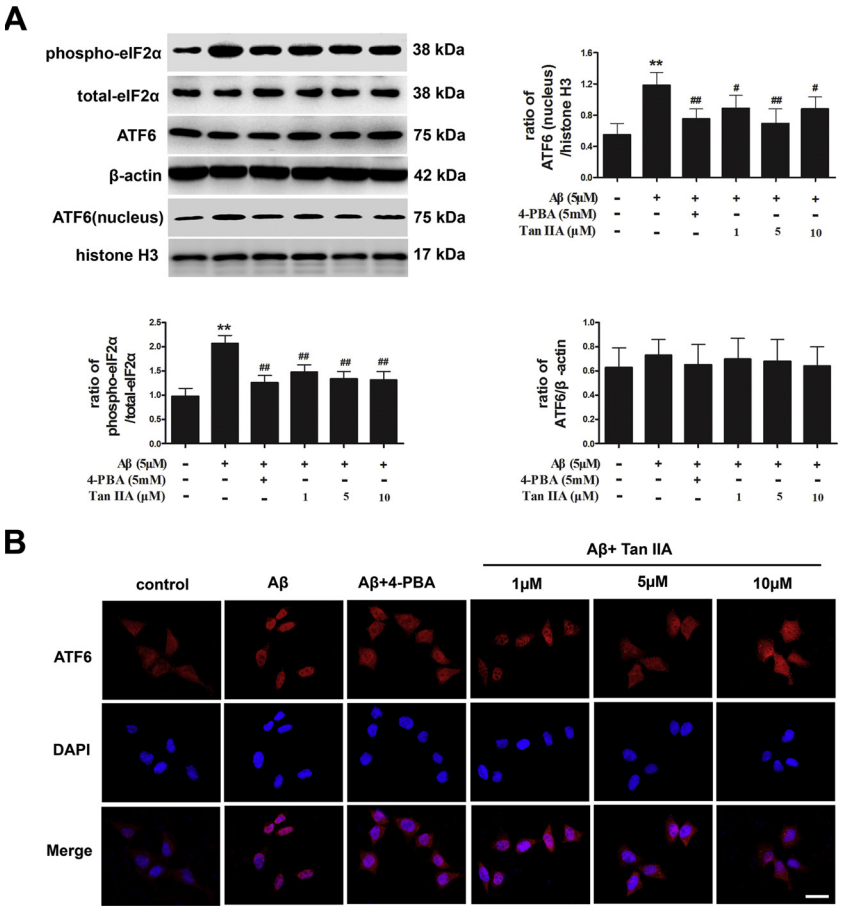

Fig. 6. Tan IIA prevented oAβ_{1-42}-induced the expression of phospho-eIF2α and ATF6 in SH-SY5Y cells. Cells were pretreated with tan IIA (1, 5, and 10 μM) for 30 min or 4-PBA (5 mM) for 6 h followed by 5 μM oAβ_{1-42} for 24 h. (A) The protein expression of eIF2α, phospho-eIF2α and ATF6 with western blotting. β-actin and histone H3 were detected for controls. (B) Immunofluorescence of ATF6 (red), the nuclear (blue) was labelled with DAPI. Scale bar is 20 μm. Results were shown as the mean ± SD. The experiments were repeated three times independently. $^{**}p < 0.01$ versus control, $^{\#}p < 0.05$ and $^{\#\#}p < 0.01$ versus oAβ_{1-42} treated cells. (For interpretation of the references to colour in this figure legend, the reader is referred to the web version of this article).

3.7. Tan IIA attenuated apoptosis-related protein in SH-SY5Y cells

The Bcl-2 family members play crucial roles in the regulation of the mitochondrial pathway of apoptosis. Bax translocates from the cytosol to the mitochondria and causes release of cytochrome *c*, followed by activates of caspase-9, which in turn activates caspase-3 (Cai et al., 2011). Caspase-3 is one of the key proteases responsible for the initiation of the caspase cascade and believed to be at the final stage of

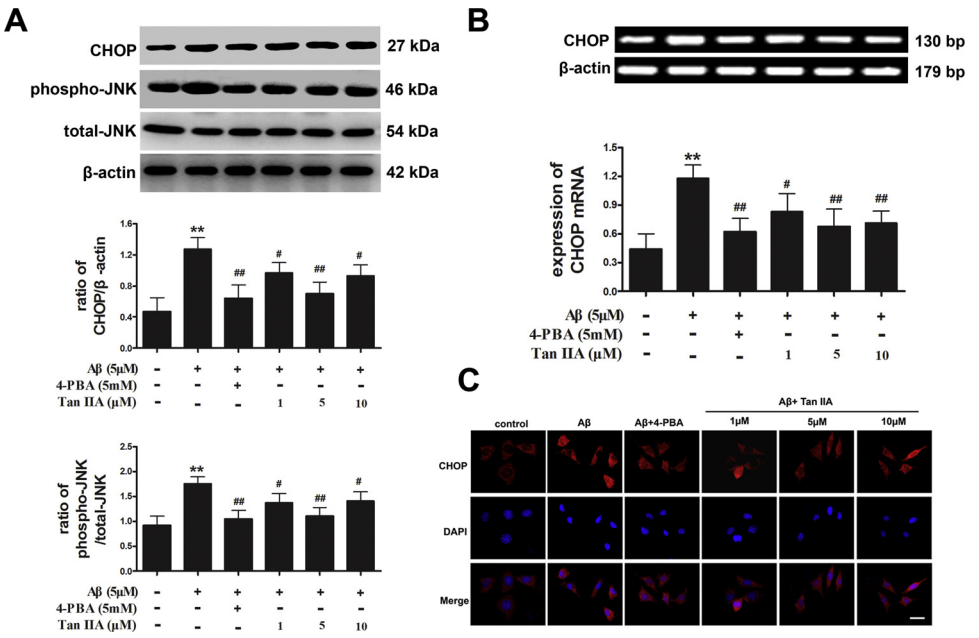

Fig. 7. Tan IIA inhibited oAβ_{1-42}-induced activation of CHOP and JNK pathways in SH-SY5Y cells. Cells were pretreated with tan IIA (1, 5, and 10 μM) for 30 min or 4-PBA (5 mM) for 6 h followed by 5 μM oAβ_{1-42} for 24 h. (A) The protein expression of CHOP, JNK and phospho-JNK with western blotting. β-actin was detected for controls. (B) The mRNA expression of CHOP with RT-PCR. β-actin was detected for controls. (C) Immunofluorescence of CHOP (red), the nuclear (blue) was labelled with DAPI. Scale bar is 20 μm. Results were shown as the mean ± SD. The experiments were repeated three times independently. $^{**}p < 0.01$ versus control, $^{\#}p < 0.05$ and $^{\#\#}p < 0.01$ versus oAβ_{1-42} treated cells. (For interpretation of the references to colour in this figure legend, the reader is referred to the web version of this article).

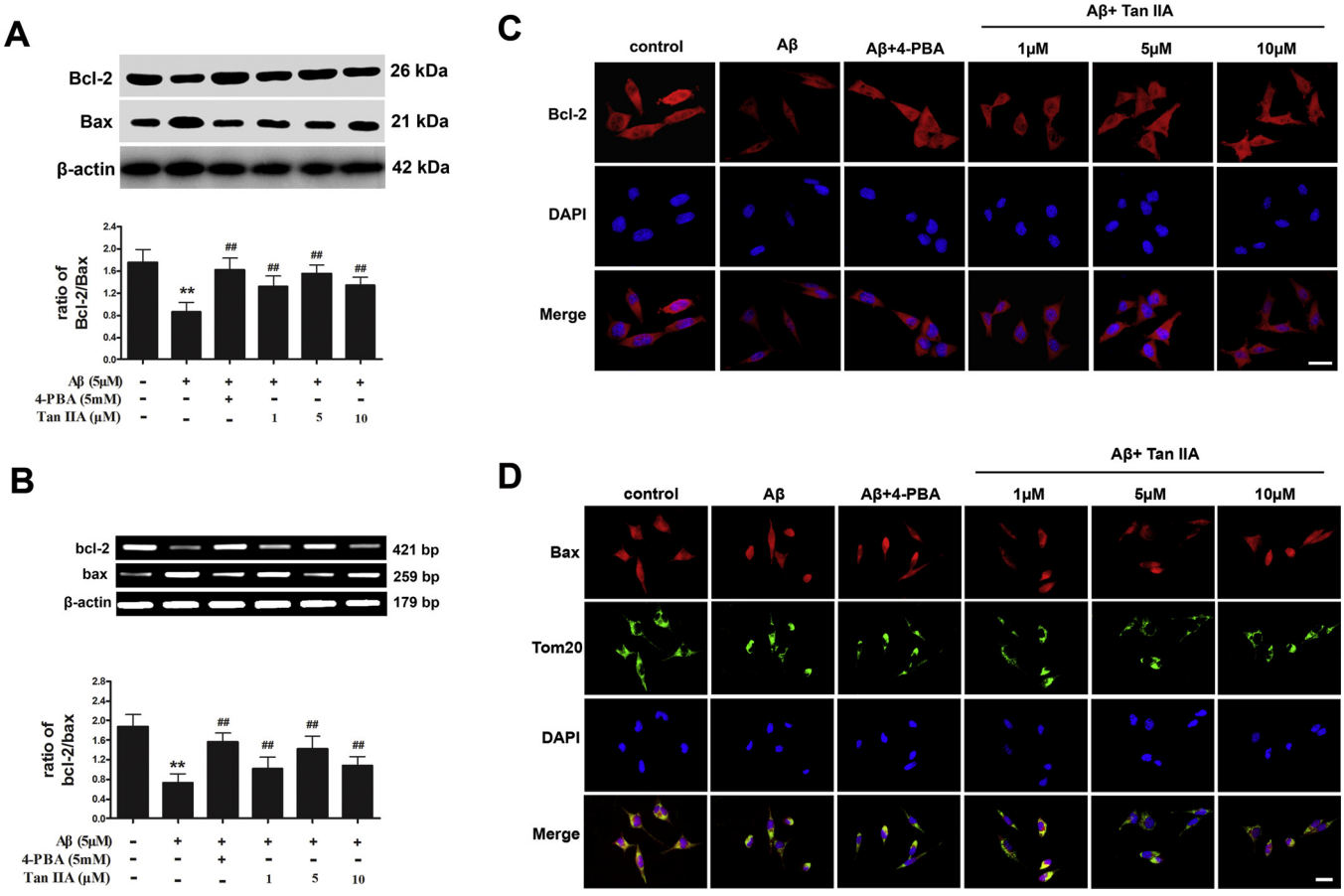

Fig. 8. Tan IIA increased oAβ_{1-42}-induced the ratio of Bcl-2/Bax in SH-SY5Y cells. Cells were pretreated with tan IIA (1, 5, and 10 μM) for 30 min or 4-PBA (5 mM) for 6 h followed by 5 μM oAβ_{1-42} for 24 h. (A) The protein expression of Bcl-2 and Bax with western blotting. β-actin was detected for controls. (B) The mRNA expression of Bcl-2 and Bax with RT-PCR. β-actin was detected for controls. (C) Immunofluorescence of Bcl-2 (red), the nuclear (blue) was labelled with DAPI. Scale bar is 20 μm. (D) Immunofluorescence of Bax (red), Tom20 (green), the nuclear (blue) was labelled with DAPI. Scale bar is 20 μm. Results were shown as the mean ± SD. The experiments were repeated three times independently. $^{**}p < 0.01$ versus control, $^{\#}p < 0.05$ and $^{\#\#}p < 0.01$ versus oAβ_{1-42} treated cells. (For interpretation of the references to colour in this figure legend, the reader is referred to the web version of this article).

apoptosis. In the present study, we examined the levels of Bcl-2 and Bax in SH-SY5Y cells by western blotting, RT-PCR and immunofluorescence assay. As shown in Fig. 8A, treatment of cells with 5 μM oAβ_{1-42} for 24 h decreased the expression of Bcl-2 and concomitantly increased Bax expression. Tan IIA (1, 5 or 10 μM) reversed the alternations of Bcl-2 and Bax expressions induced by oAβ_{1-42}, and substantially increased the ratio of Bcl-2/Bax ($p < 0.01$). The expression of Bcl-2 and Bax at the mRNA level and the immunofluorescence staining of Bcl-2 and Bax were consistent with western blotting results (Fig. 8B–D). Furthermore, in the oAβ_{1-42} treated cells, Bax were co-localized with mitochondrial marker Tom20 in dying cells. Pretreatment with tan IIA (1, 5 or 10 μM) improved this change. Meanwhile, the effects of 4-PBA on the expression of Bcl-2 and Bax were similar to tan IIA.

Next, we detected the levels of cytochrome *c,* caspase-9, cleaved caspase-9 and cleaved caspase-3 in SH-SY5Y cells. Firstly, to be sure about sample purity, GAPDH and SDHA antibodies were used as markers for cytosolic and mitochondrial fractions, respectively (Supplementary Fig. 1). Then the protein levels of cytochrome *c* in mitochondrial and cytosolic fractions were determined by western blotting. oAβ_{1-42} greatly increased the levels of cytochrome *c* in the cytosol. In the mitochondria, cytochrome *c* content was correspondingly decreased, indicating that oAβ_{1-42} increased the release of cytochrome *c* into cytosol. Consistently, treatment oAβ_{1-42} greatly increased the levels of cleaved caspase-9, cleaved caspase-3 and the activity of caspase-3/7. In contrast, tan IIA (1, 5 or 10 μM) effectively inhibited the release of cytochrome *c* and cleavage of caspase-9 and caspase-3, as well as suppressed the activity of caspase-3/7, indicating tan IIA prevented oAβ_{1-42}-induced cell apoptosis (Fig. 9A and B) ($p < 0.05$ or $p < 0.01$). In addition, an immunofluorescence assay detecting the cytochrome *c* and cleaved caspase-3 elicited the same results (Fig. 9C and D). Meanwhile, 4-PBA also attenuated the expression of cytochrome *c*, cleaved caspase-9, cleaved caspase-3 and the activity of caspase-3/7.

Furthermore, we determined MMP and ATP content in SH-SY5Y cells, which is related to mitochondrial dysfunction. As shown in Fig. 10A and B, cells exposed to oAβ_{1-42} markedly decreased MMP and ATP content, whereas these oAβ_{1-42}-induced effects were rescued to various degrees by pretreatment with tan IIA (1, 5 or 10 μM) ($p < 0.05$ or $p < 0.01$). Similar to tan IIA, 4-PBA also increased MMP and ATP content. In this experiment, 5 μM tan IIA provided more significant neuroprotection than other dosages. Taken together, these results revealed that tan IIA can protect SH-SY5Y cells against ER stress induced apoptosis through mitochondria-mediated intrinsic pathway.

4. Discussion

A few published articles have demonstrated the prevented effects of tan IIA on ER stress. In the kidneys preserved with tan IIA, the protein markers of ER stress, caspase 12, and CHOP are decreased compared with that in the kidneys maintained with Celsior solution solely (Zhang et al., 2012). In L6 myotubes, tan IIA prevented the activation of ER stress induced by tunicamycin, a widespread used activator of ER stress (Hwang et al., 2012). In cardiac fibroblasts, tan IIA treatment also weakened the radiation-induced ER stress and fibrosis damage (Gu et al., 2014). All these results demonstrated that tan IIA reduces the stimulation of ER stress, resulting in amelioration of tissue impairment. A recent study have shown that tan IIA reduced reactive oxygen species level, increased activities and protein levels of the antioxidant enzymes, increased MMP and ATP content, and inhibited glutamate-induced apoptosis through regulation of apoptosis related protein expression and MAPK activation in SH-SY5Y cells (Li et al., 2017). Although this study has demonstrated that tan IIA protects SH-SY5Y cells against glutamate toxicity. However, the role of tan IIA on ER stress mediated apoptosis and underlying mechanisms in SH-SY5Y cells is remains unclear. Our present study indicated that exposure of SH-SY5Y cells to oAβ_{1-42} (5 μM) for 24 h decreased cell viability and led to a massive apoptosis, as determined by MTT assay, morphological examination, and TUNEL staining. When the cells were preincubated with tan IIA (1, 5 or 10 μM), the cell viability, apoptotic ratio and the morphology changes of the oAβ_{1-42} treated cells were all improved. Furthermore, cells treated with oAβ_{1-42} showed that increased levels of GRP78, phospho-eIF2α and ATF6. oAβ_{1-42} also induced activation of CHOP and JNK pathways in SH-SY5Y cells. By contrast, pretreatment of tan IIA (1, 5 or 10 μM) markedly reduced ER stress related protein expression. Moreover, our results showed that oAβ_{1-42}-induced cytochrome *c* release, caspase-9 and caspase-3 activation, as well as decreasing the Bcl-2/Bax expression ratio, MMP and ATP content. However, when SH-SY5Y cells were preincubated with tan IIA (1, 5 or 10 μM), these oAβ_{1-42}-induced cellular events were reversed. Similar to tan IIA, we found that 4-PBA, an ER stress inhibitor, also has protective action against oAβ_{1-42}-induced cytotoxicity in SH-SY5Y cells. Taken together, our findings demonstrated that tan IIA can be considered as a useful neuroprotective agent for ameliorating ER stress and apoptosis triggered by oAβ_{1-42} in SH-SY5Y cells.

To confirm ER stress, we observed the expression of GRP78, the core ER regulatory protein which functions as a molecular chaperone and plays an important role in the recognition of unfolded proteins. Under normal conditions, GRP78 proteins are expressed at a low level and are bound to ER transmembrane receptors. When ER stress is triggered, the unfolded or misfolded proteins combine with free GRP78 and lead to their activation (Hetz, 2012). Therefore, GRP78 is considered to be an endoplasmic reticulum homeostat, and its up-regulation indicates the occurrence of ER stress. In the present study, GRP78 mRNA and protein levels were upregulated significantly when cells treated with oAβ_{1-42}, indicating ER stress activation. However, tan IIA (1, 5 or 10 μM) significantly decreased GRP78 expression at the mRNA and protein levels. ER stress is sensed by the luminal domains of three ER transmembrane proteins: PERK, ATF6 and IRE1. PERK is a transmembrane kinase which dimerizes and autophosphorylates when stress is sensed. Its main function is to regulate protein synthesis through phosphorylation of eIF2α. ATF6 is a transcription factor which gets shuttled to the Golgi for its ER stress-mediated activation. Translocation of the processed form of ATF6 to the nucleus results in the upregulation of UPR homeostatic effectors involved in protein folding, processing, and degradation (Fonseca et al., 2011). To further explore the inhibitory effects of tan IIA on ER stress signaling pathway induced by oAβ_{1-42} in SH-SY5Y cells, we tested the levels of phospho-eIF2α and ATF6 in each group. In our study, oAβ_{1-42} upregulated the levels of phospho-eIF2α, while tan IIA (1, 5 or 10 μM) markedly down-regulated its expression in SH-SY5Y cells. Meanwhile, tan IIA (1, 5 or 10 μM) significantly downregulated the protein levels of ATF6 in the nuclear fractions compared to the oAβ_{1-42} group. All of the findings indicated that tan IIA can inhibit ER stress by inhibiting PERK/eIF2α, and ATF6 pathways.

When ER functions are severely impaired, apoptotic signals are triggered to eliminate the damaged cells (Kaufman, 1999). CHOP, as a basic leucine zipper transcription factor, which is regulated under the PERK, IRE1, and ATF6 arms of the UPR, assumes the best indicator of pro-apoptotic phase in ER-stressed cells (Kennedy et al., 2015; Rao et al., 2013; Sari et al., 2010; Yao et al., 2015; Zhao et al., 2018). So, prevention of the initiation of pro-apoptotic events through down-regulation of CHOP partially protects ER stress. In this study, we found that the levels of CHOP protein and mRNA are upregulated in oAβ_{1-42} treated cells, but significantly inhibited by tan IIA (1, 5 or 10 μM). It has been reported that JNK activation is required in the ER stress of islet beta cells and JNK-mediated signaling pathways lead to apoptotic UPR during ER stress (Chan et al., 2015; Lakshmanan et al., 2011). In the present study, the results revealed that the phospho-JNK was progressively increased in oAβ_{1-42} treated cells. Pretreatment of tan IIA (1, 5 or 10 μM) significantly attenuated the phospho-JNK. These findings demonstrated that tan IIA inhibits ER stress-induced apoptosis at least partly through suppression of CHOP and JNK pathways.

Bcl-2 family proteins appear to be the downstream executors of CHOP-mediated apoptotic signals. Overexpression of CHOP has been

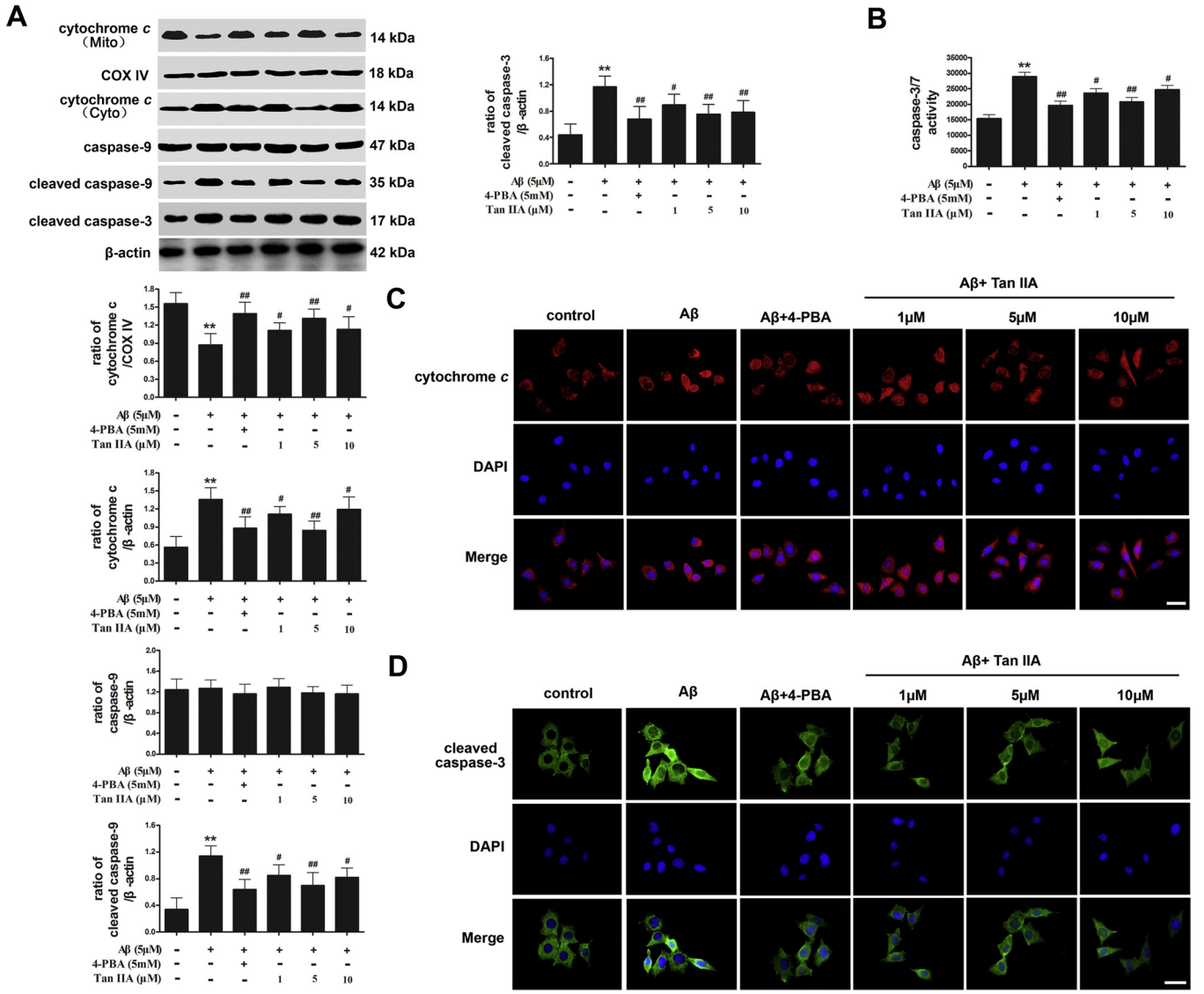

Fig. 9. Tan IIA attenuated oAβ_{1-42}-induced the levels of cytochrome *c*, cleaved caspase-9, cleaved caspase-3 and the activity of caspase-3/7 in SH-SY5Y cells. Cells were pretreated with tan IIA (1, 5, and 10 μM) for 30 min or 4-PBA (5 mM) for 6 h followed by 5 μM oAβ_{1-42} for 24 h. (A) The protein levels of cytochrome *c* in mitochondrial and cytosolic fractions, caspase-9, cleaved caspase-9 and cleaved caspase-3 in total protein extracts were analyzed by western blotting. β-actin and COX IV were detected for controls. (B) Determination of caspase-3/7 activity. (C) Immunofluorescence of cytochrome *c* (red), the nuclear (blue) was labelled with DAPI. Scale bar is 20 μm. (D) Immunofluorescence of cleaved caspase-3 (green), the nuclear (blue) was labelled with DAPI. Scale bar is 20 μm. Results were shown as the mean ± SD. The experiments were repeated three times independently. $^{**}p < 0.01$ versus control, $^{\#}p < 0.05$ and $^{\#\#}p < 0.01$ versus oAβ_{1-42} treated cells (For interpretation of the references to colour in this figure legend, the reader is referred to the web version of this article).

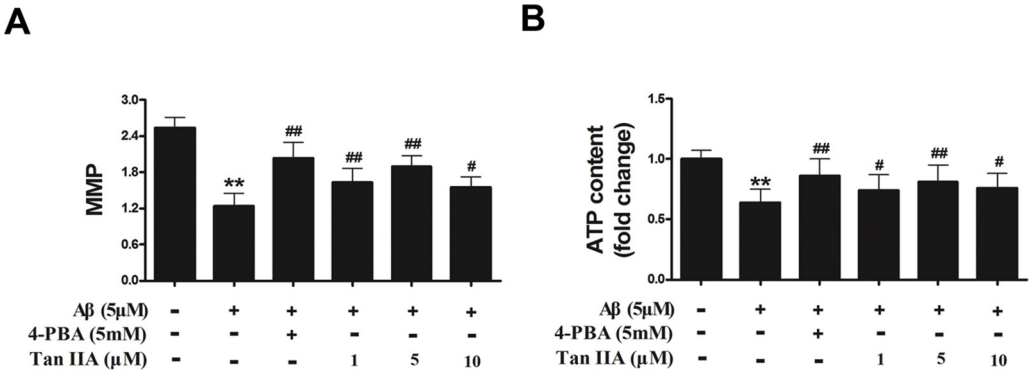

Fig. 10. Tan IIA increased oAβ_{1-42}-induced MMP and ATP content in SH-SY5Y cells. Cells were pretreated with tan IIA (1, 5, and 10 μM) for 30 min or 4-PBA (5 mM) for 6 h followed by 5 μM oAβ_{1-42} for 24 h. (A) Determination of MMP. (B) Determination of ATP content. Results were shown as the mean ± SD. The experiments were repeated three times independently. $^{**}p < 0.01$ versus control, $^{\#}p < 0.05$ and $^{\#\#}p < 0.01$ versus oAβ_{1-42} treated cells.

shown to mediate the decrease of Bcl-2 protein and perturbation of the cellular redox state (Chen et al., 2018; Gu et al., 2010; Matsumoto et al., 1996; McCullough et al., 2001; Oyadomari and Mori, 2004). In addition, JNK activation through the IRE1 pathway may lead to Bcl-2 and Bcl-xL phosphorylation and their subsequent inactivation (Davis, 2000; Fan et al., 2000). Whether CHOP or JNK mediated, cell death induced by ER stressors has been widely shown to occur through the mitochondrial pathway of apoptosis. In the mitochondrial pathway, the loss of MMP due to mitochondrial outer membrane permeabilization represents an important event that is controlled by the Bcl-2 proteins. The Bcl-2 family comprises both proapoptotic members, including BH3-only proteins and the multidomain effector proteins Bak and Bax, as well as antiapoptotic members (such as Bcl-2 and Bcl-xL). BH3-only proteins trigger Bax/Bak activation. Once activated, Bak and Bax can initiate a pore in the outer mitochondrial membrane, resulting in the detachment of proteins like cytochrome *c* from the mitochondrial intermembrane space and their release into the cytosol (Heinicke et al., 2018; Pecot et al., 2016). Upon release, cytochrome *c* facilitates apoptosome formation, thus causing caspase activation and execution of apoptotic cell death (Zhan et al., 2015). Meanwhile, BH3-only proteins trigger cell death by neutralizing antiapoptotic Bcl-2 family members. In this investigation, we found that tan IIA (1, 5 or 10 μM) reversed the alternations of Bcl-2 and Bax expressions induced by oAβ_{1-42}, and substantially restored the ratio of Bcl-2/Bax in SH-SY5Y cells. Additionally, pretreatment with tan IIA ameliorated the oAβ_{1-42}-induced increase in Bax level at the mitochondria. We also found that oAβ_{1-42} caused the release of cytochrome *c* from the mitochondria to cytosol, an attributive process during induction of apoptosis. In contrast, tan IIA (1, 5 or 10 μM) treatment strongly inhibited the release of cytochrome *c*. Accordingly, tan IIA (1, 5 or 10 μM) blocked the expression of cleaved caspase-9 and cleaved caspase-3, as well as suppressed the activity of caspase-3/7. Furthermore, tan IIA (1, 5 or 10 μM) pretreatment significantly increased MMP and ATP content. Collectively, these results revealed that tan IIA is able to prevent ER stress induced apoptosis via mitochondria-mediated intrinsic pathway.

A number of studies have shown an upregulation of ER stress markers in AD models, and many groups have reported upregulation of the ER stress response in post-mortem human AD brains (Barbero-Camps et al., 2014; Ma et al., 2013; Mouton Liger et al., 2012; Yoon et al., 2012). From the point of view of Ca^{2+} homeostasis anomalies or protein misfolding in AD, ER stress could be regarded as a plausible mechanism leading to cell injury. Danshen and its active components, such as tan IIA have been used in clinical practice as drugs with efficient blood-brain barrier penetration (Yu et al., 2011), and thus, may attenuate the development of cognitive impairment by suppressing ER stress induced apoptosis.

In summary, we demonstrated that tan IIA protects SH-SY5Y cells against oAβ_{1-42}-induced apoptosis and the possible mechanisms. Our results showed that oAβ_{1-42} decreased cell survival, induced occurrence of excess ER stress and apoptosis. However, these oAβ_{1-42}-induced changes were significantly prevented by co-treatment with tan IIA through attenuating the expression of ER stress markers GRP78, eIF2α and ATF6, modulating the CHOP and JNK signaling pathways, decreasing the expression of cytochrome *c*, cleaved caspase-9 and cleaved caspase-3, suppressing the activity of caspase-3/7, increasing the ratio of Bcl-2/Bax, MMP and ATP content. In the present study, we have used only an in vitro model. Therefore, the role of tan IIA on ER stress induced apoptosis needs to be further confirmed by using different models, such as in a different *in vitro* model (primary neurons) or *in vivo* model (APPsw/PS1dE9 mice).

Conflict of interest statement

The authors declare that there are no conflicts of interest.

Acknowledgments

This work was supported by the Natural Science Foundation of China (81500928, 81571251), Natural Science Basic Research Plan in Shaanxi Province of China (2018JM7056). China Postdoctoral Science Foundation (2017T100758, 2016M590955), Postdoctoral Science Foundation of Shaanxi Province (2016BSHYDZZ04), Open Innovation Research Project (2017BKKF-Int.12, 2017BKKF-Int.19).

Appendix A. Supplementary data

Supplementary material related to this article can be found, in the online version, at doi:https://doi.org/10.1016/j.biocel.2018.12.011.

References

Akaberi, M., Iranshahi, M., Mehri, S., 2016. Molecular signaling pathways behind the biological effects of salvia species diterpenes in neuropharmacology and cardiology. Phytother. Res. 30, 878–893.
Barbero-Camps, E., Fernandez, A., Baulies, A., Martinez, L., Fernandez-Checa, J.C., Colell, A., 2014. Endoplasmic reticulum stress mediates amyloid beta neurotoxicity via mitochondrial cholesterol trafficking. Am. J. Pathol. 184, 2066–2081.
Bertolotti, A., Zhang, Y.H., Hendershot, L.M., Harding, H.P., Ron, D., 2000. Dynamic interaction of BiP and ER stress transducers in the unfolded-protein response. Nat. Cell Biol. 2, 326–332.
Cai, X., Zhang, H., Tong, D., Tan, Z., Han, D., Ji, F., et al., 2011. Corosolic acid triggers mitochondria and caspase-dependent apoptotic cell death in osteosarcoma MG-63 cells. Phytother. Res. 25, 1354–1361.
Cai, N., Zhao, X., Jing, Y., Sun, K., Jiao, S., Chen, X., et al., 2014. Autophagy protects against palmitate-induced apoptosis in hepatocytes. Cell Biosci. 4, 28.
Chafekar, S.M., Hoozemans, J.J.M., Zwart, R., Baas, F., Scheper, W., 2007. A beta(1-42) induces mild endoplasmic reticulum stress in an aggregation state-dependent manner. Antioxid. Redox Signal. 9, 2245–2254.
Chan, J.Y., Luzuriaga, J., Maxwell, E.L., West, P.K., Bensellam, M., Laybutt, D.R., 2015. The balance between adaptive and apoptotic unfolded protein responses regulates beta-cell death under ER stress conditions through XBP1, CHOP and JNK. Mol. Cell. Endocrinol. 413, 189–201.
Chen, X., Bisschops, M.M.M., Agarwal, N.R., Ji, B.Y., Shanmugavel, K.P., Petranovic, D., 2017. Interplay of energetics and ER stress exacerbates Alzheimer's amyloid-beta (A beta) toxicity in yeast. Front. Mol. Neurosci. 10, 232.
Chen, W., Chan, Y., Wan, W., Li, Y., Zhang, C., 2018. Abeta1-42 induces cell damage via RAGE-dependent endoplasmic reticulum stress in bEnd.3 cells. Exp. Cell Res. 362, 83–89.
Choi, G.E., Lee, S.J., Lee, H.J., Ko, S.H., Chae, C.W., Han, H.J., 2017. Membrane-associated effects of glucocorticoid on BACE1 upregulation and A beta generation: involvement of lipid raft-mediated CREB activation. J. Neurosci. 37, 8459–8476.
Chromy, B.A., Nowak, R.J., Lambert, M.P., Viola, K.L., Chang, L., Velasco, P.T., et al., 2003. Self-assembly of A beta (1-42) into globular neurotoxins. Biochemistry 42, 12749–12760.
Costa, R.O., Lacor, P.N., Ferreira, I.L., Resende, R., Auberson, Y.P., Klein, W.L., et al., 2012. Endoplasmic reticulum stress occurs downstream of GluN2B subunit of N-methyl-d-aspartate receptor in mature hippocampal cultures treated with amyloid-ss oligomers. Aging Cell 11, 823–833.
Dahlgren, K.N., Manelli, A.M., Stine, W.B., Baker, L.K., Krafft, G.A., LaDu, M.J., 2002. Oligomeric and fibrillar species of amyloid-beta peptides differentially affect neuronal viability. J. Biol. Chem. 277, 32046–32053.
Davis, R.J., 2000. Signal transduction by the JNK group of MAP kinases. Cell 103, 239–252.
Dong, H., Mao, S., Wei, J., Liu, B., Zhang, Z., Zhang, Q., et al., 2012. Tanshinone IIA protects PC12 cells from beta-amyloid(25-35)-induced apoptosis via PI3K/Akt signaling pathway. Mol. Biol. Rep. 39, 6495–6503.
Duran-Aniotz, C., Martinez, G., Hetz, C., 2014. Memory loss in Alzheimer's disease: are the alterations in the UPR network involved in the cognitive impairment? Front. Aging. Neurosci. 6 (8).
Evans, N.A., Facci, L., Owen, D.E., Soden, P.E., Burbidge, S.A., Prinjha, R.K., et al., 2008. A beta(1-42) reduces synapse number and inhibits neurite outgrowth in primary cortical and hippocampal neurons: a quantitative analysis. J. Neurosci. Methods 175, 96–103.
Fan, M.Y., Goodwin, M., Vu, T., Brantley-Finley, C., Gaarde, W.A., Chambers, T.C., 2000. Vinblastine-induced phosphorylation of Bcl-2 and Bcl-X-L is mediated by JNK and occurs in parallel with inactivation of the Raf-1/MEK/ERK cascade. J. Biol. Chem. 275, 29980–29985.
Ferreira, S.T., Klein, W.L., 2011. The A beta oligomer hypothesis for synapse failure and memory loss in Alzheimer's disease. Neurobiol. Learn. Mem. 96, 529–543.
Fonseca, S.G., Gromada, J., Urano, F., 2011. Endoplasmic reticulum stress and pancreatic beta-cell death. Trends Endocrinol. Metab. 22, 266–274.
Gerakis, Y., Hetz, C., 2017. Emerging roles of ER stress in the etiology and pathogenesis of Alzheimer's disease. FEBS J. 285, 995–1011.
Ghaderi, S., Ahmadian, S., Soheili, Z.S., Ahmadieh, H., Samiei, S., Kheitan, S., et al., 2018. AAV delivery of GRP78/BiP promotes adaptation of human RPE cell to ER stress. J. Cell. Biochem. 119, 1355–1367.

Gu, X., Li, K., Laybutt, D.R., He, M.L., Zhao, H.L., Chan, J.C.N., et al., 2010. Bip overexpression, but not CHOP inhibition, attenuates fatty-acid-induced endoplasmic reticulum stress and apoptosis in HepG2 liver cells. Life Sci. 87, 724–732.
Gu, J., Li, H.L., Wu, H.Y., Gu, M., Li, Y.D., Wang, X.G., et al., 2014. Sodium tanshinone IIA sulfonate attenuates radiation-induced fibrosis damage in cardiac fibroblasts. J. Asian Nat. Prod. Res. 16, 941–952.
Guo, X., Lv, J., Lu, J., Fan, L., Huang, X., Hu, L., et al., 2018. Protopanaxadiol derivative DDPU improves behavior and cognitive deficit in AD mice involving regulation of both ER stress and autophagy. Neuropharmacology 130, 77–91.
Hardy, J., Allsop, D., 1991. Amyloid deposition as the central evet in the etiology of Alzheimers-disease. Trends Pharmacol. Sci. 12, 383–388.
Heinicke, U., Haydn, T., Kehr, S., Vogler, M., Fulda, S., 2018. BCL-2 selective inhibitor ABT-199 primes rhabdomyosarcoma cells to histone deacetylase inhibitor-induced apoptosis. Oncogene. https://doi.org/10.1038/s41388-018-0212-5.
Hetz, C., 2012. The unfolded protein response: controlling cell fate decisions under ER stress and beyond. Nat. Rev. Mol. Cell Biol. 13, 89–102.
Hosoi, T., Sasaki, M., Baba, S., Ozawa, K., 2009. Effect of pranoprofen on endoplasmic reticulum stress in the primary cultured glial cells. Neurochem. Int. 54, 1–6.
Hu, Y., Li, X.C., Wang, Z.H., Luo, Y., Zhang, X., Liu, X.P., et al., 2016. Tau accumulation impairs mitophagy via increasing mitochondrial membrane potential and reducing mitochondrial Parkin. Oncotarget 7, 17356–17368.
Hwang, S.L., Yang, J.H., Jeong, Y.T., Kim, Y.D., Li, X., Lu, Y., et al., 2012. Tanshinone IIA improves endoplasmic reticulum stress-induced insulin resistance through AMP-activated protein kinase. Biochem. Biophys. Res. Commun. 430, 1246–1252.
Jeon, S., Bose, S., Hur, J., Jun, K., Kim, Y.K., Cho, K.S., et al., 2011. A modified formulation of Chinese traditional medicine improves memory impairment and reduces A beta level in the Tg-APPswe/PS1dE9 mouse model of Alzheimer's disease. J. Ethnopharmacol. 137, 783–789.
Jiang, P., Li, C., Xiang, Z., Jiao, B., 2014. Tanshinone IIA reduces the risk of Alzheimer's disease by inhibiting iNOS, MMP-2 and NF-kappa B p65 transcription and translation in the temporal lobes of rat models of Alzheimer's disease. Mol. Med. Rep. 10, 689–694.
Kaufman, R.J., 1999. Stress signaling from the lumen of the endoplasmic reticulum: coordination of gene transcriptional and translational controls. Genes Dev. 13, 1211–1233.
Kennedy, D., Samali, A., Jaeger, R., 2015. Methods for studying ER stress and UPR markers in human cells. In stress responses: methods and protocols. Methods Mol. Biol. 1292, 3–18.
Kittelberger, K.A., Piazza, F., Tesco, G., Reijmers, L.G., 2012. Natural amyloid-beta oligomers acutely impair the formation of a contextual fear memory in mice. PLoS One 7, e29940.
Kokubo, H., Kayed, R., Glabe, C.G., Yamaguchi, H., 2005. Soluble A beta oligomers ultrastructurally localize to cell processes and might be related to synaptic dysfunction in Alzheimer's disease brain. Brain Res. 1031, 222–228.
Kong, D., Liu, Q., Xu, G., Huang, Z., Luo, N., Huang, Y., et al., 2017. Synergistic effect of tanshinone IIA and mesenchymal stem cells on preventing learning and memory deficits via anti-apoptosis, attenuating tau phosphorylation and enhancing the activity of central cholinergic system in vascular dementia. Neurosci. Lett. 637, 175–181.
LaFerla, F.M., Green, K.N., Oddo, S., 2007. Intracellular amyloid-beta in Alzheimer's disease. Nat. Rev. Neurosci. 8, 499–509.
Lakshmanan, A.P., Thandavarayan, R.A., Palaniyandi, S.S., Sari, F.R., Meilei, H., Giridharan, V.V., et al., 2011. Modulation of AT-1R/CHOP-JNK-Caspase12 pathway by olmesartan treatment attenuates ER stress-induced renal apoptosis in streptozotocin-induced diabetic mice. Eur. J. Pharm. Sci. 44, 627–634.
Lee, D.Y., Lee, K.S., Lee, H.J., Kim, D.H., Noh, Y.H., Yu, K., et al., 2010. Activation of PERK signaling attenuates A beta-mediated ER stress. PLoS One 5, e10489.
Li, H., Han, W., Wang, H., Ding, F., Xiao, L., Shi, R., et al., 2017. Tanshinone IIA inhibits glutamate-induced oxidative toxicity through prevention of mitochondrial dysfunction and suppression of MAPK activation in SH-SY5Y human neuroblastoma cells. Oxid. Med. Cell. Longev. 4517486, 1–13.
Lim, C.S., Han, J.S., 2018. The anti-oxidant xanthorrhizol prevents amyloid-beta-induced oxidative modification and inactivation of neprilysin. Biosci. Rep. 38, 1.
Liu, C., Wu, Y., Zha, S., Liu, M., Wang, Y., Yang, G., et al., 2016. Treatment effects of tanshinone IIA against intracerebroventricular streptozotocin induced memory deficits in mice. Brain Res. 1631, 137–146.
Ma, T., Trinh, M.A., Wexler, A.J., Bourbon, C., Gatti, E., Pierre, P., et al., 2013. Suppression of eIF2 alpha kinases alleviates Alzheimer's disease-related plasticity and memory deficits. Nat. Neurosci. 16, 1299–U1185.
Maione, F., Piccolo, M., De Vita, S., Chini, M.G., Cristiano, C., De Caro, C., et al., 2017. Down regulation of pro-inflammatory pathways by tanshinone IIA and cryptotanshinone in a non-genetic mouse model of Alzheimer's disease. Pharmacol. Res. 129, 482–490.
Matsumoto, M., Minami, M., Takeda, K., Sakao, Y., Akira, S., 1996. Ectopic expression of CHOP (GADD153) induces apoptosis in M1 myeloblastic leukemia cells. FEBS Lett. 395, 143–147.
McCullough, K.D., Martindale, J.L., Klotz, L.O., AW, T.Y., Holbrook, N.J., 2001. Gadd153 sensitizes cells to endoplasmic reticulum stress by down-regulating Bc12 and perturbing the cellular redox state. Mol. Cell. Biol. 21, 1249–1259.
Mouton Liger, F., Paquet, C., Dumurgier, J., Bouras, C., Pradier, L., Gray, F., et al., 2012. Oxidative stress increases BACE1 protein levels through activation of the PKR-eIF2 alpha pathway. Biochim. Biophys. Acta Mol. Basis Dis. 1822, 885–896.
Musiek, E.S., Holtzman, D.M., 2015. Three dimensions of the amyloid hypothesis: time, space and' wingmen'. Nat. Neurosci. 18, 800–806.
Oddo, S., Caccamo, A., Smith, I.F., Green, K.N., LaFerla, F.M., 2006. A dynamic relationship between intracellular and extracellular pools of A beta. Am. J. Pathol. 168, 184–194.
Oyadomari, S., Mori, M., 2004. Roles of CHOP/GADD153 in endoplasmic reticulum stress. Cell Death Differ. 11, 381–389.
Pecot, J., Maillet, L., Le Pen, J., Vuillier, C., Trecesson, Sd.C., Fetiveau, A., et al., 2016. Tight sequestration of BH3 proteins by BCL-xL at subcellular membranes contributes to apoptotic resistance. Cell Rep. 17, 3347–3358.
Qian, Y.H., Xiao, Q., Xu, J., 2012. The protective effects of tanshinone IIA on beta-amyloid protein (1-42)-induced cytotoxicity via activation of the Bcl-xL pathway in neuron. Brain Res. Bull. 88, 354–358.
Rao, J., Qin, J., Qian, X., Lu, L., Wang, P., Wu, Z., et al., 2013. Lipopolysaccharide preconditioning protects hepatocytes from ischemia/reperfusion injury (IRI) through inhibiting ATF4-CHOP pathway in mice. PLoS One 8, e65568.
Sadeghi, A., Ebrahimi, S.S.S., Golestani, A., Meshkani, R., 2017. Resveratrol ameliorates palmitate-induced inflammation in skeletal muscle cells by attenuating oxidative stress and JNK/NF-kappa B pathway in a SIRT1-Independent mechanism. J. Cell. Biochem. 118, 2654–2663.
Sakono, M., Zako, T., 2010. Amyloid oligomers: formation and toxicity of A beta oligomers. FEBS J. 277, 1348–1358.
Sari, F.R., Watanabe, K., Thandavarayan, R.A., Harima, M., Zhang, S., Muslin, A.J., et al., 2010. 14-3-3 Protein protects against cardiac endoplasmic reticulum stress (ERS) and ERS-initiated apoptosis in experimental diabetes. J. Pharmacol. Sci. 113, 325–334.
Seo, E.J., Fischer, N., Efferth, T., 2017. Phytochemicals as inhibitors of NF-kappaB for treatment of Alzheimer's disease. Pharmacol. Res. 129, 262–273.
Sharma, M., Urano, F., Jaeschke, A., 2012. Cdc42 and Rac1 are major contributors to the saturated fatty acid-stimulated JNK pathway in hepatocytes. J. Hepatol. 56, 192–198.
Shi, L.L., Yang, W.N., Chen, X.L., Zhang, J.S., Yang, P.B., Hu, X.D., et al., 2012. The protective effects of tanshinone IIA on neurotoxicity induced by beta-amyloid protein through calpain and the p35/Cdk5 pathway in primary cortical neurons. Neurochem. Int. 61, 227–235.
Song, S., Kim, S.Y., Hong, Y.M., Jo, D.G., Lee, J.Y., Shim, S.M., et al., 2003. Essential role of E2-25K/Hip-2 in mediating amyloid-beta neurotoxicity. Mol. Cell 12, 553–563.
Takahashi, R.H., Almeida, C.G., Kearney, P.F., Yu, F.M., Lin, M.T., Milner, T.A., et al., 2004. Oligomerization of Alzheimer's beta-amyloid within processes and synapses of cultured neurons and brain. J. Neurosci. 24, 3592–3599.
Tarantino, G., Caputi, A., 2011. JNKs, insulin resistance and inflammation: a possible link between NAFLD and coronary artery disease. World J. Gastroenterol. 17, 3785–3794.
Teodoro, T., Odisho, T., Sidorova, E., Volchuk, A., 2012. Pancreatic beta-cells depend on basal expression of active ATF6 alpha-p50 for cell survival even under nonstress conditions. Am. J. Physiol. Cell Physiol. 302, C992–C1003.
Tseng, B.P., Green, K.N., Chan, J.L., Blurton-Jones, M., LaFerla, F.M., 2008. A beta inhibits the proteasome and enhances amyloid and tau accumulation. Neurobiol. Aging 29, 1607–1618.
Urano, F., Wang, X.Z., Bertolotti, A., Zhang, Y.H., Chung, P., Harding, H.P., et al., 2000. Coupling of stress in the ER to activation of JNK protein kinases by transmembrane protein kinase IRE1. Science 287, 664–666.
Urra, H., Dufey, E., Lisbona, F., Rojas-Rivera, D., Hetz, C., 2013. When ER stress reaches a dead end. Biochim. Biophys. Acta Mol. Cell Res. 1833, 3507–3517.
Vattem, K.M., Wek, R.C., 2004. Reinitiation involving upstream ORFs regulates ATF4 mRNA translation in mammalian cells. Proc. Natl. Acad. Sci. U. S. A. 101, 11269–11274.
Wang, Q., Yu, X., Patal, K., Hu, R., Chuang, S., Zhang, G., et al., 2013. Tanshinones inhibit amyloid aggregation by amyloid-beta peptide, disaggregate amyloid fibrils, and protect cultured cells. ACS Chem. Neurosci. 4, 1004–1015.
Wortel, I.M.N., van der Meer, L.T., Kilberg, M.S., van Leeuwen, F.N., 2017. Surviving stress: modulation of ATF4-mediated stress responses in normal and malignant cells. Trends Endocrinol. Metab. 28, 794–806.
Yang, W.N., Ma, K.G., Qian, Y.H., Zhang, J.S., Feng, G.F., Shi, L.L., et al., 2015. Mitogen-activated protein kinase signaling pathways promote low-density lipoprotein receptor-related protein 1-mediated internalization of beta-amyloid protein in primary cortical neurons. Int. J. Biochem. Cell Biol. 64, 252–264.
Yao, S., Tian, H., Miao, C., Zhang, D.W., Zhao, L., Li, Y., et al., 2015. D4F alleviates macrophage-derived foam cell apoptosis by inhibiting CD36 expression and ER stress-CHOP pathway. J. Lipid Res. 56, 836–847.
Yao, Y., Chen, X.C., Bao, Y.T., Wu, Y.S., 2017. Puerarin inhibits ss-amyloid peptide 1-42-induced tau hyperphosphorylation via the Wnt/ss-catenin signaling pathway. Mol. Med. Rep. 16, 9081–9085.
Yoon, S.O., Park, D.J., Ryu, J.C., Ozer, H.G., Tep, C., Shin, Y.J., et al., 2012. JNK3 perpetuates metabolic stress induced by A beta peptides. Neuron 75, 824–837.
Yu, P.F., Wang, W.Y., Eerdun, G., Wang, T., Zhang, L.M., Li, C., et al., 2011. The role of P-glycoprotein in transport of danshensu across the blood-brain barrier. Evid. Based Complement. Altern. Med. 1–5 2011.
Zhan, M., Usman, I.M., Sun, L., Kanwar, Y.S., 2015. Disruption of renal tubular mitochondrial quality control by myo-inositol oxygenase in diabetic kidney disease. J. Am. Soc. Nephrol. 26, 1304–1321.
Zhang, X.M., He, D.Q., Xu, L.H., Ling, S.C., 2012. Protective effect of tanshinone IIA on rat kidneys during hypothermic preservation. Mol. Med. Rep. 5, 405–409.
Zhao, Y., Fang, Y., Zhao, H., Li, J., Duan, Y., Shi, W., et al., 2018. Chrysophanol inhibits endoplasmic reticulum stress in cerebral ischemia and reperfusion mice. Eur. J. Pharmacol 818, 1–9.